

Scaling laws in granular continuous avalanches in a rotating drum

N. Sepúlveda, G. Krstulovic, S. Rica*

*Departamento de Física, Facultad de Ciencias Físicas y Matemáticas de la Universidad de Chile,
Blanco Encalada 2008, Santiago, Chile*

Available online 9 June 2005

Abstract

We study the front shape of avalanches produced in a rotating two-dimensional drum partially filled with small glass beads. We focus our work on the study of the length and shape of granular fronts, in particular how they do scale in terms of the physical parameters involved. A single scaling law for the length is found. This scaling law is also relevant for the behavior of the full shape of the fronts. More than 300 different fronts shape, for different values of the parameters collapse into an universal curve.

© 2005 Elsevier B.V. All rights reserved.

Keywords: Granular matter; Granular flows; Avalanches

Since pioneering works by Bagnold [1] granular flows under gravity have been considered in many different contexts and geometries. The relevance of this phenomenon is great because of the industrial process of various materials, and natural catastrophes such as landslides, clay and snow avalanches [2]. In spite of a long history of experiments on granular flows, the phenomenon encounters several fundamental difficulties in its theory and application.

More than a decade ago, Jaeger et al. [3] and Rajchenbach [4] have recognized that a continuous avalanche regime could be realized in a rotating drum geometry, as one increases the rotation speed of the drum. Indeed for low angular frequencies an

*Corresponding author.

E-mail address: rica@dfi.uchile.cl (S. Rica).

intermittent regime is observed [3], meanwhile as one increases the rotating speed, a continuous avalanche regime is established [4].

As soon as the drum starts to rotate, the bulk of beads climb-up with the drum until the upper beads loose their stability falling down, producing an avalanche. Ultimately, those rolling beads arrive at the bottom of the cell loosing its motion, then they are carried up again, creating a continuous cycle. Inside the cell grains experiment two different regimes: while grains are ascending the inter-particle distance remains fixed, like in a solid, meanwhile falling grains, that is the avalanche, behave like a fluid. During the whole process there is a continuous exchange of particles between the solid and fluid part. A kinetic model describing these processes was proposed in Ref. [5]. However, the model predicts a parabolic shape of the rolling grains at the interface [6] instead of the characteristic S shape profile observed in experiments [4]. Later, Zik et al. [7] studied segregation in a rotating drum describing the observed S shape of the interface for a half-filled rotating drum. More recently, Ottino and collaborators [8] reported measurements of the shear speed in the rolling layer and Rajchenbach [9] modifies Bagnold stress to explain constant shear rate for dense and rapid flows.

In this article we report a rotating drum experiment partially filled with glass beads. We study the stationary avalanches finding scaling laws for the length and the full profile of the fronts when the angular velocity, the drum radius, the volume filled by the beads and the size of the particles vary.

Experiment. The experimental setup consists of a two-dimensional Hele–Shaw rotating drum partially filled with small glass beads (Fig. 1a). The two faces of the drum were built in Plexiglas, each one with a furrow inside where a rubber o-ring is placed making uniform cell spacing about $b = 1.8$ mm. We have worked with three different cell radii (a): 4.5, 12.5 and 16.5 cm. The cell can rotate around an axis perpendicular to gravity driven by a motor with constant power and a system of a set of pulleys allowing us to explore a large range of angular velocity between 0.003 and 6 rad/s.

We will focus our study on the length and shape of the front, in particular how do fronts scale in terms of the physical parameters involved? Those are: the angular velocity ω , the radius a of the drum, the size D of the particles and the initial filling

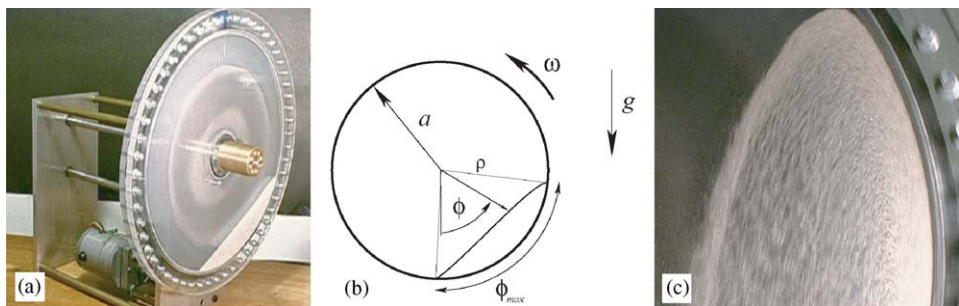


Fig. 1. (a) Experimental setup. (b) Scheme of the experiment, parameters and variables. (c) Grains flying parabolically like in a “ball mill.”

fraction. Although the distance b between both faces of the drum remains constant in the full set of experiments, we could anticipate a dependence on this parameter because of dimensional analysis. This dependence is strange because the plexiglas being smoother than the rubber o-ring, one may expect that friction among the cell sides would not be relevant, therefore, one should not expect a dependence of scaling laws on the thickness b .

We summarize in the following table, the range of variations of the parameters keeping in mind that the angular frequency ω and the filling fraction (determined by the initial angular arc ϕ_0) extended at rest (Fig. 1b) are varied continuously. For all the grains, the repose angle happens to be almost constant and $\theta_r \approx 32^\circ$.

| ω (rad/s) | ϕ_0 (deg) | a (cm) | D (μm) | b (mm) | $\omega\sqrt{a/g}$ | a/b | b/D |
|------------------|----------------|----------|-----------------------|----------|--------------------|-------|---------|
| 0.01 | 40 | 4.5 | 75–150 | 1.8 | 6×10^{-4} | 25 | 24–12 |
| ↓ | ↓ | 12.5 | 150–250 | | ↓ | 70 | 12–7.2 |
| | | 16.5 | 350–420 | | | 92 | 5–4.3 |
| 3 | 110 | | 420–500 | | 0.4 | | 4.3–3.6 |

In the experiment it is not possible to use the complete range of ω given by our setup, because there are two natural bounds. For large ω , if $\omega^2 > g/a$ the system acts as a centrifuge, moreover, before that a non-steady behavior arises when grains placed in the upper part are thrown parabolically from the border to the interior (Fig. 1c). This behavior is the basic principle of a “ball mill” in the mining industry: because of a large effective friction between the rubber at the bottom and the granular bed, the material could be stucked inside the cylinder for large angles. The material does not slip downhill as in an avalanche, but they do fly inside the cell. Finally, for tiny grains air-drag is also important at large angular speeds. On the other hand, for very small ω , only discrete avalanches can be seen [3,4], those avalanches present an intermittent behavior [3]. This last rotating frequency is about $\omega_r \sim 0.02$ rad/seg.

Measurements were made using a digital video camera working at a standard speed of 30 frame/s, from the movies one gets the full color profile (see Fig. 2, left), then each picture is treated in grayscale with Photoshop. Next, the figures are transformed into a binary scale using Matlab and, finally, the data for the profile interface are obtained and processed (see Fig. 2, right).

Scaling law for the front length. Using dimensionless parameters the only possible general law for the profile angular length is

$$\phi_{max} = f_1 \left(\omega \sqrt{\frac{a}{g}}, \frac{b}{D}, \frac{a}{b}, \phi_0 \right). \quad (1)$$

The function $f_1(\cdot)$ should be rather complex, thus we try to explore a particular limit, mainly $a/b \gg 1$, and $\omega\sqrt{a/g} \ll 1$ but keeping $\omega a > \sqrt{gD}$ and finite, that is an intermediate asymptotic. It will be desirable to have the limit of a small filling

fraction $\phi_0 \ll 1$ to recover the essential aspects of an avalanche over a flat surface, however, that limit is difficult to reach, e.g. for $\phi_0 = 40^\circ$ the profile is almost undistinguishable. On the other hand, a large electrostatic charge per particle appears in such a small amount of grains. Finally, the limit $b/D \gg 1$ is only partially reached because we are limited by electrostatic effects appearing in very small particles and the increase of b needs a different cell that will change dramatically the rough boundary.

In order to settle relation (1) we use the fact that there is only one dimensionless parameter involving ω , so first, the measurements were made for fixed particle diameter $D = 75\text{--}150 \mu\text{m}$, initial filling fraction $\phi_0 = 65^\circ$ and cell radius $a = 16.5 \text{ cm}$ while the angular frequency, ω , varying between the range considered. Over a large number of experimental points (see Fig. 3, left \bullet), a linear regression of their

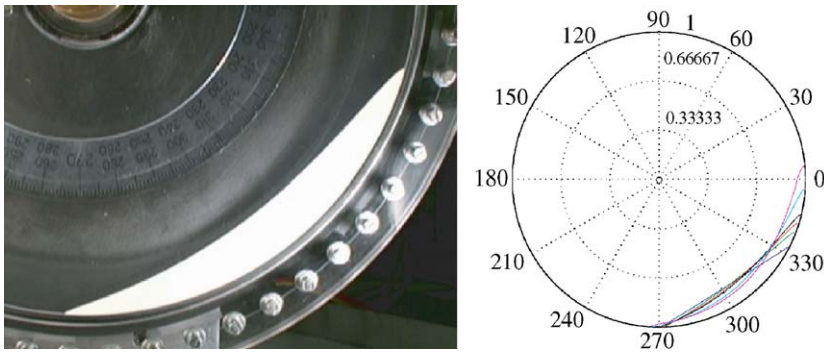


Fig. 2. Left: a digital photograph of a front for $\omega\sqrt{a/g} = 0.025$, $a = 16.5 \text{ cm}$, $D = 70\text{--}150 \mu\text{m}$. Right: a polar plot ρ/a of different fronts obtained at (end front increases with ω) $\omega = 0$, $\omega = 0.08 \text{ s}^{-1}$, $\omega = 0.13 \text{ s}^{-1}$, $\omega = 0.18 \text{ s}^{-1}$, $\omega = 0.47 \text{ s}^{-1}$ and $\omega = 0.59 \text{ s}^{-1}$. Note that the position of front of the avalanche remains almost at the same place: $270^\circ \pm 5^\circ$, independently of the rotating frequency.

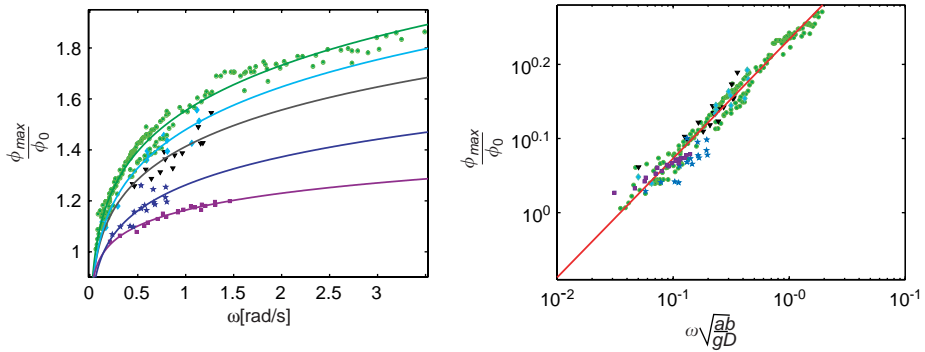


Fig. 3. Left: summary for the profile length ϕ_{max}/ϕ_0 for different initial filling fractions, cell radii, particle diameters as function of ω . \bullet : $a = 16.5 \text{ cm}$, $D = 75\text{--}150 \mu\text{m}$; \blacklozenge : $a = 16.5 \text{ cm}$, $D = 150\text{--}250 \mu\text{m}$; \blacktriangledown : $a = 16.5 \text{ cm}$, $D = 320\text{--}450 \mu\text{m}$; \blackstar : $a = 12.5 \text{ cm}$, $D = 320\text{--}450 \mu\text{m}$; \blacksquare : $a = 4.5 \text{ cm}$, $D = 320\text{--}450 \mu\text{m}$. Right: full collapse for all data the front length ϕ_{max}/ϕ_0 vs. $\omega\sqrt{ab/gD}$.

logarithms with 95% confidence bounds leads the law $\phi_{max} \sim \omega^{1/6 \pm 0.012}$ with an excellent correlation coefficient of 0.995. Naturally, this power law has no sense in the limit $\omega \rightarrow 0$, which is clearly omitted in our study because $\omega a > \sqrt{gD}$. Next, we study the dependance of $f_1(\cdot)$ varying the other parameters a and ϕ_0 , but keeping constant the particle diameter D . We have noticed that if one plots ϕ_{max}/ϕ_0 as a function of $\omega\sqrt{a/g}$ for different values of a and ϕ_0 all different points collapse in a single curve. Writing $\phi_{max}/\phi_0 = \tilde{f}_1(\omega\sqrt{a/g}, b/D, a/b, \phi_0)$ we can deduce that there is no (or very weak) dependence of a/b and ϕ_0 in the function $\tilde{f}_1(\cdot)$.

Finally, we have done experiments under the same experimental procedure with glass particles of different sizes as in the table. We see that the scaling $\phi_{max}/\phi_0 \sim (\omega\sqrt{a/g})^{1/6}$ fails as we change D (see Fig. 3, left). Thus, \tilde{f}_1 depends weakly on the parameter b/D for the range considered.

The best fit of all data is the following (see Fig. 3, right)

$$\frac{\phi_{max}}{\phi_0} = (1.77 \pm 0.07) \left(\frac{b}{D}\right)^{1/12 \pm 0.008} \left(\omega\sqrt{\frac{a}{g}}\right)^{1/6 \pm 0.012}. \quad (2)$$

That indicates that $\omega\sqrt{ab/gD}$ should be the relevant dimensionless parameter. No existing theory or model [1,9] reveals such a parameter up-to-date.

Scaling law for the shape of the fronts. In this section, we will study the full shape of the profile of the avalanche. Dimensional analysis indicates that the profile dependence should be (in polar coordinates, see Fig. 1b)

$$\frac{\rho(\phi)}{a} = f_2\left(\omega\sqrt{\frac{a}{g}}, \frac{b}{D}, \frac{a}{b}, \phi_0; \phi\right) \quad (3)$$

being $f_2(\cdot)$ a new universal function. However, because of the mass conservation we could guess a possible dependence of $f_2(\cdot)$ on the similarity law (1) or (2) in the region of parameters considered stated in the previous section. If the area of the profile is conserved, something to be checked a posteriori, one has that the area at rest and that for arbitrary ω are the same. Let be $h = a - \rho$, thus we have

$$\frac{a^2}{2}(\phi_0 - \sin \phi_0) = \frac{1}{2} \int_{\phi_{min}}^{\phi_{max}} (a^2 - (a - h(\phi))^2) d\phi \approx a \int_0^{\phi_{max}} h(\phi) d\phi, \quad (4)$$

where the integration is realized over the angles of the profile. The last approximation considers $h \ll a$ and we have set $\phi_{min} \approx 0$ after Fig. 2, right. Making the change of variable $\phi = \phi_{max} \tilde{\phi}$ one transforms ϕ into the interval $[0, 1]$. Redefining the profile as (hereafter f_1 stands by $\tilde{f}_1(\omega\sqrt{a/g}, b/D, a/b, \phi_0)$)

$$\frac{\rho(\phi)}{a} = 1 - \frac{1}{2\tilde{f}_1} \left(1 - \frac{\sin \phi_0}{\phi_0}\right) \tilde{h}(\tilde{\phi} = \phi/\phi_0 \tilde{f}_1). \quad (5)$$

Here $\tilde{h}(\tilde{\phi})$ is a new universal function that will describe the shape of any front after the proper scaling. Conservation of mass implies that $\int_0^1 \tilde{h}(\tilde{\phi}) d\tilde{\phi} = 1$.

In Fig. 4, left, we see many different fronts: $h/a = 1 - \rho/a$ vs. polar angle ϕ for different parameters ω, a, L_0, D . On the right-hand side of Fig. 4 we have the plot of the front scaled using relation (5), there we can see a good collapse into the universal

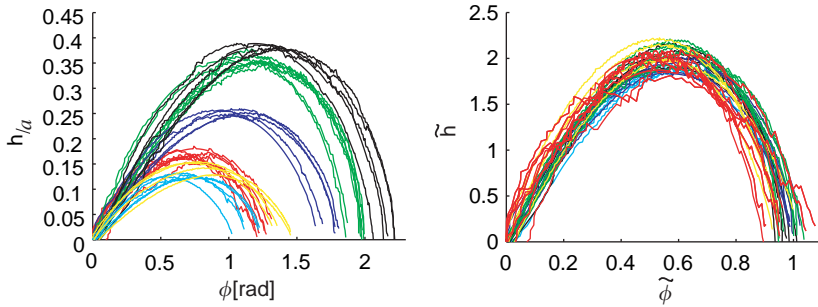


Fig. 4. Left: different front profiles for different parameters value. Right: full collapse of the universal front $\tilde{h}(\tilde{\phi})$.

curve $\tilde{h}(\tilde{\phi})$ within a range of confidence of 10%. The collapse is good only for $\omega\sqrt{a/g} \leq 0.07$. That means that for large rotation frequencies the area is no longer conserved somewhat reasonably because of the dilatance of the grain layers at high rotation speed.

Conclusion. We report a large number of measurements of the size and shape of fronts of avalanches produced by a rotating two-dimensional drum. We have found a scaling law (2) for the size of the front. Moreover, because of mass conservation this scaling law determines the full shape of fronts characterized by an universal curve plotted in Fig. 4, right. Hundred different fronts, for different values of the parameters, collapse into this universal curve.

Finally, the authors acknowledge the grant Fondecyt 1020359 and Fondap 11980002 (Chile), they would like to thank S. Contreras and M.A. Soto for their hospitality at the Biophysics laboratory, and they are grateful to N. Fraysse (Nice) and I. Aranson (Argonne) for gentle grains provision and R. Walker for a careful reading of the manuscript.

References

[1] R.A. Bagnold, Proc. Roy. Soc. (London) A 225 (1954) 49, reprinted in The Physics of Sediment Transport by Wind and Water, American Society of Civil Engineers, New York, 1988, p. 114.
 [2] E.J. Hopfinger, Ann. Rev. Fluid Mech. 15 (1983) 47.
 [3] H.M. Jaeger, C. Liu, S. Nagel, Phys. Rev. Lett. 62 (1989) 40.
 [4] J. Rajchenbach, Phys. Rev. Lett. 65 (1990) 2221.
 [5] J.P. Bouchaud, M. Cates, Ravi Prakash, S.F. Edwards, J. Phys. I 4 (1994) 1383.
 [6] P.-G. de Gennes, C.R. Acad. Sci., Ser. Iib 321 (1995) 501.
 [7] O. Zik, et al., Phys. Rev. Lett. 73 (1994) 644.
 [8] N. Jain, J.M. Ottino, R.M. Lueptow, Phys. Fluids 14 (2002) 572.
 [9] J. Rajchenbach, Phys. Rev. Lett. 90 (2003) 144302.